Observation of phonon hopping in radial vibrational modes of trapped ions

Shinsuke Haze, Yusuke Tateishi, Atsushi Noguchi, Kenji Toyoda, and Shinji Urabe

Graduate School of Engineering Science, Osaka University, 1-3 Machikaneyama, Toyonaka, Osaka 560-8531, Japan

We observed phonon hopping by using the radial vibrational motion of trapped ions and we investigated the properties of radial mode phonons, which can be used for quantum simulation of the Hubbard model. This study represents an essential step toward realizing a physical implementation of the Bose-Hubbard model with trapped ions.

Quantum simulation of many-body systems opens the way to investigate intriguing phenomena in solid-state physics such as high-temperature superconductivity. Trapped ions are promising systems for quantum simulations and several experiments have been demonstrated, including the simulation of Ising spin models [1,2]. The radial vibrational modes of ions have been used to generate an effective Ising interaction [2,3] and tunable spin-spin couplings have been measured [4].

Radial motion of ions can also be applied to the quantum simulation of the Bose-Hubbard model (BHM), in which localized bosons hop between sites [5]. The radial phonons of trapped ions are suitable for simulating such a system because the radial trapping potential can be made much larger than the Coulomb interaction so that radial phonons can be considered to be locally trapped phonons in each ion [6,7]. Thus, when trapped ions are used to simulate the BHM, radial phonons act as bosons at each site and the Coulomb interaction induces phonon hopping.

Trapped ions have the advantages of good controllability of the internal and external degrees of freedom and the ability to address single ions in the ion chain. When simulating the BHM with trapped ions, these advantages allow us to realize unique physical situations in the BHM.

In this Rapid Communication, we report the observation of phonon hopping dynamics in radial vibrational modes of two trapped ions. This study is an essential step toward realizing the physical implementation of the BHM with trapped ions.

Similar experiments have been performed recently in which phonon energy is exchanged between remotely trapped ions in a double-well potential [8,9]. Such an energy exchange can be used to transmit quantum information between remote ions.

Trapped ions in a linear Paul trap form a linear chain in one direction when the radial confinement is stronger than the axial confinement so that the motion can be decomposed into three-dimensional vibrations in the axial (z) and radial (x and y) directions. The Hamiltonian that governs motion in one of the radial directions (which we take to be the y direction in this study) can be written as

$$H_y = \sum_{i=1,2} \frac{P_i^2}{2m} + \sum_{i=1,2} \frac{1}{2} m\omega_y^2 y_i^2 - \frac{1}{2} \frac{e^2}{|z_1 - z_2|^3}(y_1 - y_2)^2.$$

(1)

Here, we consider the case of two ions for simplicity. y_i and z_i are the spatial coordinates and P_i is the momentum of the ith ion in the ion chain. m is the ion mass and ω_y is

the trap frequency in the y direction. The first two terms in the Hamiltonian represent the kinetic energy and the trap potential and the last term is the Coulomb interaction.

Equation (1) can be rewritten in terms of local phonon operators as [6,7]

$$H_y = \sum_{i=1,2} \hbar\left(\omega_y - \frac{\kappa}{2}\right)a_i^\dagger a_i + \frac{\hbar\kappa}{2}(a_1 a_2^\dagger + a_1^\dagger a_2),$$

(2)

where

$$\kappa = \frac{e^2}{d_0^3 m\omega_y}.$$

(3)

a_i and $a_i^\dagger$ are, respectively, the annihilation and creation operators of the y mode phonons of the ith ion, $d_0 = |z_1 - z_2|$ is the interior distance in the axial direction, and κ represents the phonon hopping rate. The first term is the trap potential in the y direction; it contains a harmonic potential correction due to the Coulomb interaction. The second term represents hopping of phonons between ions 1 and 2.

To derive Eq. (2), the phonon number nonconserving terms a_i^2, $a_i^{\dagger 2}$, $a_1 a_2$, and $a_1^\dagger a_2^\dagger$, are neglected in the rotating wave approximation. This approximation is valid for radial-mode phonons because the trap potential is much larger than the Coulomb potential [6].

For two ions, the hopping interaction couples $|n\rangle_1|n+1\rangle_2$ and $|n+1\rangle_1|n\rangle_2$, which causes phonon energy to be exchanged between the ions at the phonon hopping rate κ. Here, $|n\rangle_i$ represents the Fock state of the ith ion, where n is the phonon quantum number.

Phonon hopping can also be explained in terms of the normal modes of the radial vibrational motion. The Hamiltonian given by Eq. (2) can be rewritten in terms of two eigenmodes whose frequencies are separated by $\hbar\kappa$. The creation operators of these modes are $a_c^\dagger = (a_1^\dagger + a_2^\dagger)/\sqrt{2}$ and $a_c^\dagger = (a_1^\dagger - a_2^\dagger)/\sqrt{2}$, which correspond to the center-of-mass (c.m.) mode and the rocking mode, respectively. For one-phonon excitation, the two eigenstates are $(|1\rangle|0\rangle \pm |0\rangle|1\rangle)/\sqrt{2}$. When one phonon is excited in the local mode, the nonstationary state of $|1\rangle|0\rangle$ evolves into the state $|\psi(t)\rangle = e^{-i\omega_y t}[\cos(\kappa t/2)|1\rangle|0\rangle - i \sin(\kappa t/2)|0\rangle|1\rangle]$, which shows that the phonon hops at a rate of κ.

To observe phonon hopping, we use the radial mode of two $^{40}Ca^+$ ions in a linear trap where the radio-frequency and dc electric fields give radial and axial confinement, respectively. The radio-frequency signal is fed to the trap electrode through

a helical resonator that has a resonance frequency of 25 MHz. In our setup, the distance between ions and the electrode is 600 μm. When only a radio-frequency field is applied in the radial directions, the secular frequencies for the radial directions are degenerate due to the rotational symmetry. To lift this degeneracy and address a specific vibrational mode, we apply a dc voltage to a diagonal pair of trap electrodes that are segmented into three parts. The trap frequency in each direction is $(\omega_x,\omega_y,\omega_z)/2\pi = (3.36,3.17,0.82)$ MHz and the corresponding interior distance in the axial direction is 6.4 μm. A detailed description of the trap apparatus and the laser configuration is described in our previous study [10].

Two-step laser cooling employing Doppler cooling using the $S_{1/2}$-$P_{1/2}$ transition and sideband cooling using the $S_{1/2}$-$D_{5/2}$ quadrupole transition enables ground-state cooling of all the vibrational modes. The mean phonon number of the c.m. modes in each direction after sideband cooling is $(\langle n_x\rangle,\langle n_y\rangle,\langle n_z\rangle) = (0.08,0.08,0.11)$ under typical experimental conditions. In the case of the rocking mode, the mean phonon number of the x and y modes are measured to be below 0.09 after sideband cooling. The inverse of the ion heating rates of x,y, and z modes (c.m.) are also measured to be $[83(7),97(20),488(120)]$ ms/quanta using the method described in Ref. [11].

The laser beam for the quadrupole transition (729 nm) is oriented 60°, 60°, and 45° relative to the x, y, and z directions, respectively, and the projection of the wave vector in each direction is $(k_x,k_y,k_z) = (\frac{1}{2},\frac{1}{2},\frac{1}{\sqrt{2}})|\mathbf{k}|$. $\mathbf{k}$ is the wave vector of the 729-nm laser. In our setup, ions are equally illuminated by the 729-nm laser radiation and the error of the intensity at the ions is less than 5%.

Phonon hopping is observed using the following steps (the experimental sequence is shown in Fig. 1). (1) All the six vibrational modes of two ions comprising the c.m. and rocking modes of the radial and axial vibrations are cooled to near the ground state by sideband cooling at $d_0 = 6.4$ μm ($\omega_z = 2\pi \times$ 820 kHz). (2) The interior distance is dynamically increased by ramping down the dc voltage for axial trapping. The ramping profile is exponential. The ramping time, which we define here as the time when the voltage is decreased to $1/e$ from the initial value, is 1.2 ms and the axial trap frequency is adiabatically decreased for 5 ms. (3) A π pulse that is resonant with the blue sideband transition is applied to one of the ions to prepare the initial phonon state of $|0\rangle_1|1\rangle_2$. Immediately after this, a 854-nm laser pulse that is nearly resonant with the $D_{5/2}$-$P_{3/2}$ transition is applied to pump the internal state to $S_{1/2}$. (4) A

delay time with no laser interaction is inserted to observe phonon hopping; the Coulomb interaction induces coupling between $|0\rangle_1|1\rangle_2$ and $|1\rangle_1|0\rangle_2$ with a coupling strength κ. (5) A laser pulse for exciting the sideband transition is applied to the ions to estimate the mean phonon number of each ion by comparing the excitation probabilities of the red and blue sideband transitions [12]. (6) The ion separation is restored to the initial separation by increasing the dc voltage for axial trapping. The ions are irradiated by light from the 397-nm laser and their fluorescence is detected by an intensified charge-coupled-device camera to determine the internal states of the individual ions.

In step (3), a tightly focused laser beam (full width at half maximum of 22 μm), which is detuned by 50 GHz from the $D_{5/2}$-$P_{3/2}$ transition, is applied to generate a spatial inhomogeneity of the ac Stark shift to $D_{5/2}$. It enables us to manipulate the state of the individual ions and to create a local phonon in the desired ion. The same method is described in our previous study [13]. Moreover, the pulse width for local phonon creation is shorter than the phonon hopping time $1/\kappa$, so that phonon hopping to the other ion can be prevented during phonon creation.

For this reason, the hopping rate must be smaller than $\eta_y\Omega$ to prepare an appropriate initial state. Here, η_y is the Lamb-Dicke parameter and Ω is the Rabi frequency of the quadrupole transition. However, $\eta_y\Omega$ is limited to $\sim$12 kHz due to technical limitations on the laser power. It is thus necessary to adjust the ion spacing so as to satisfy $\kappa < \eta_y\Omega$; this requires that d_0 be greater than 13 μm. The corresponding axial trap frequency ω_z is below $2\pi \times 280$ kHz and the Lamb-Dicke parameter η_z is above 0.13. However, under these conditions, sideband cooling of the axial motion is not efficient because the axial motion is not well within the Lamb-Dicke region characterized by $\eta_z\sqrt{n_z} \ll 1$ after Doppler cooling. Therefore, we selected the above-mentioned scheme that involves a dynamical change in the axial potential.

Figure 2 shows a result showing phonon hopping between two ions. The horizontal and vertical axes represent the hopping time and the mean phonon number of each ion,
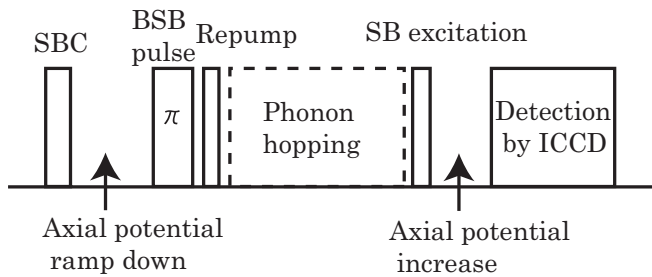

FIG. 1. Experimental time sequence for observing phonon hopping (SBC: sideband cooling; BSB: blue sideband; ICCD: intensified charge coupled device).
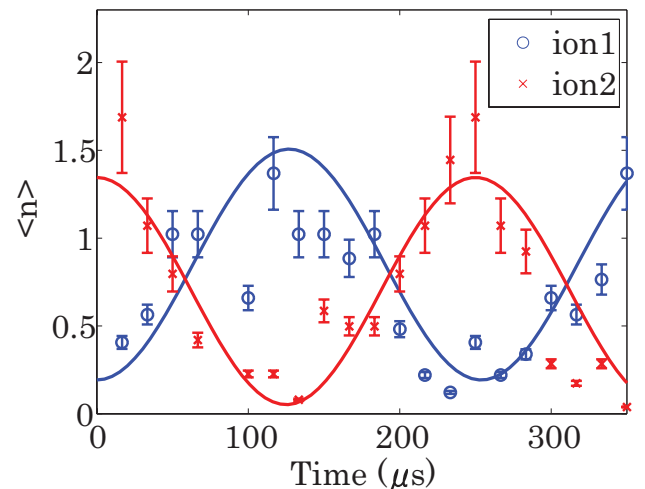

FIG. 2. (Color online) Observed phonon hopping dynamics. The horizontal and vertical axes represent the hopping time and the mean phonon number of each ion, respectively.

respectively. The hopping time is varied by changing the delay time in step (4). The trap frequency in the radial direction is $\omega_y = 2\pi \times 3.23$ MHz and the ion separation is 18.9 μm. The ion separation is estimated using the relationship $d_0 = (\frac{e^2}{4\pi\epsilon_0 m\omega_z^2})^{1/3}\frac{2.018}{2^{0.559}}$ [14,15], where we used the experimentally measured value of $\omega_z = 2\pi \times 161$ kHz.

Figure 2 reveals sinusoidal oscillations in the mean phonon number of each ion. The oscillations of ions 1 and 2 are out of phase with each other, indicating that energy is exchanged between the two ions by coherent phonon hopping. By fitting the data with a sinusoidal function the hopping rate is estimated to be $\kappa = 2\pi \times 4.0(2)$ kHz. The hopping rate is calculated to be $\kappa = 2\pi \times 4.02$ kHz from Eq. (3), which agrees with the experimentally measured value.

In the ideal case, the mean phonon number will oscillate between 0 and 1; in contrast, the result in Fig. 2 exhibits an offset in the residual phonon number. We speculate that this is mainly due to ion heating by the rf noise from the trap electrodes during the dynamical changing the ion distance in step (2), which leads to the displacement of the ion's position from the null point of the rf potential. The measured mean phonon number immediately after step (2) is typically about 0.23.

The pulse width for preparing the initial phonon state is 40 μs, which is shorter than the hopping time $1/\kappa$. The expected value for the phonon number of ion 1 at the end of the pulse is calculated to be 9.5×10^{-2}. This is obtained by solving the Schrödinger equation for the following Hamiltonian, which includes the ion-laser interaction and phonon hopping, $H = \frac{\hbar\eta\Omega}{2}(\sigma_2^+ a_2^\dagger + \sigma_2^- a_2) + \frac{\hbar\kappa}{2}(a_1^\dagger a_2 + a_1 a_2^\dagger)$. Here, σ_2^+ and σ_2^- respectively represent the raising and lowering operators for the quadrupole transition of ion 2. $\eta\Omega = 2\pi \times 12.5$ kHz and $\kappa = 2\pi \times 4.0$ kHz are used in the calculation. Such unwanted phonon excitation can be suppressed by reducing the ratio of κ to $\eta\Omega$.
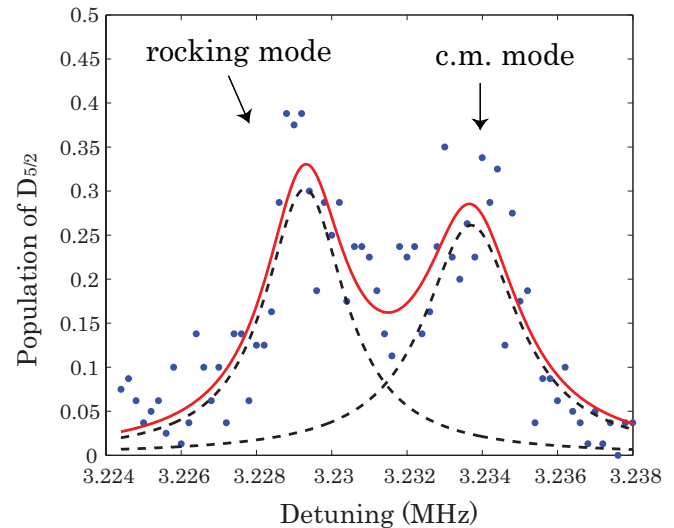
FIG. 4. (Color online) Measured spectrum of the center-of-mass and rocking modes (blue sideband transition) when $\omega_y/2\pi = 3.23$ MHz and the interion distance is 17.8 μm. The splitting of the two modes was estimated to be 4.4(2) kHz by fitting the data.

To investigate the dependence of the hopping rate on the interion distance in Eq. (3), we measured the hopping dynamics for various ion separations while keeping the radial trap frequency ($\omega_y = 2\pi \times 3.23$ MHz). Figure 3 shows a plot of the obtained hopping rates as a function of the interion distance. The dashed line represents a curve calculated using Eq. (3); it fits the experimental data well.

The energy splitting of the normal modes (c.m. and rocking) of radial vibrations is identical to the hopping rate. Figure 4 shows a measured two-mode spectrum of the blue sideband transition for an ion separation of 17.8 μm and for $\omega_y = 2\pi \times 3.23$ MHz. This is taken with a sequence similar to the case of the phonon hopping, with steps (1), (2), (5), and (6), where the frequency of the pulse in step (5) is varied. The excitation pulse width is 300 μm. The solid line is the fitting curve, which is a sum of two Gaussian functions (dashed line). The mode splitting estimated from the fitting is 4.4(2) kHz; it is plotted in Fig. 3. We conjecture that the deviation from the calculation results is due to the slow fluctuation of the rf drive during the measurement sequence, which takes more than 5 min, and that leads to slow and small drift of hundreds of hertz of the radial trap frequency.

The limiting factor of the fidelity in these experiments is ion heating during the dynamic change of the axial trap potential. A possible way to reduce this heating is to alter the laser beam configuration such that the wave vector of the 729-nm laser is orthogonal to the axial trap direction; this would allow the dynamical change in the potential to be omitted, preventing unwanted phonon creation.

It is necessary to generate the phonon-phonon interaction to realize quantum simulation of the BHM. One possible scheme for this is to introduce an optical standing wave in the radial direction that is far from resonance to induce anharmonicity in the radial trap potential [6,7]. For ^{40}Ca$^+$ ions, it is possible to use a laser that is off resonance from the $S_{1/2}$-$P_{1/2}$ or $D_{5/2}$-$P_{3/2}$ dipole transition. It is expected to be possible to generate a
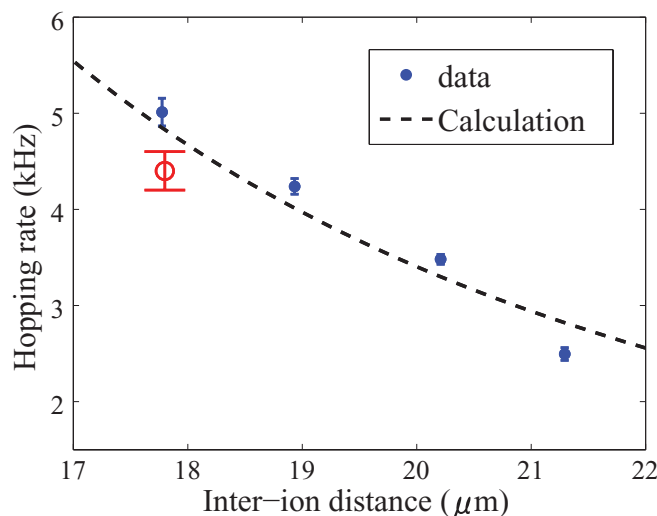

FIG. 3. (Color online) Hopping rate as a function of the interion distance. The solid circles represent data obtained by measuring the phonon hopping dynamics. The open circle represents the result of a measurement of the mode splitting (see Fig. 4).

phonon-phonon interaction of 5 kHz using a 150-mW laser beam with a beam radius of 40 μm that is detuned by 100 GHz from the $S_{1/2}$-$P_{1/2}$ transition. Moreover, it is possible to mimic the phonon-phonon interaction by using the laser-ion interaction, as proposed in Ref. [16], where trapped ions were considered theoretically for simulating physical systems consisting of a coupled-cavity array or interacting polaritons described by the Jaynes-Cummings-Hubbard model.

In conclusion, we have observed phonon hopping by using the radial vibrational modes of trapped ions and we have investigated the character of radial-mode phonons. The next challenges toward realizing the quantum simulation of many-body systems are to generate the phonon-phonon interaction and to increase the number of ions.

[1] A. Friedenauer, H. Schmitz, J. Glueckert, D. Porras, and T. Schaetz, Nat. Phys. **4**, 757 (2008).

[2] K. Kim, M.-S. Chang, S. Korenblit, R. Islam, E. E. Edwards, J. K. Freericks, G.-D. Lin, L.-M. Duan, and C. Monroe, Nature (London) **465**, 590 (2010).

[3] R. Islam, E. E. Edwards, K. Kim, S. Korenblit, C. Noh, H. Carmichael, G.-D. Lin, L.-M. Duan, C.-C. Joseph Wang, J. K. Freericks, and C. Monroe, Nat. Commun. **2**, 377 (2011).

[4] K. Kim, M.-S. Chang, R. Islam, S. Korenblit, L.-M. Duan, and C. Monroe, Phys. Rev. Lett. **103**, 120502 (2009).

[5] M. P. A. Fisher, P. B. Weichman, G. Grinstein, and D. S. Fisher, Phys. Rev. B **40**, 546 (1989).

[6] D. Porras and J. I. Cirac, Phys. Rev. Lett. **93**, 263602 (2004).

[7] X.-L. Deng, D. Porras, and J. I. Cirac, Phys. Rev. A **77**, 033403 (2008).

[8] M. Harlander, R. Lechner, M. Brownnutt, R. Blatt, and W. Hänsel, Nature (London) **471**, 200 (2011).

[9] K. R. Brown, C. Ospelkaus, Y. Colombe, A. C. Wilson, D. Leibfried, and D. J. Wineland, Nature (London) **471**, 196 (2011).

[10] K. Toyoda, S. Haze, R. Yamazaki, and S. Urabe, Phys. Rev. A **81**, 032322 (2010).

[11] R. J. Epstein, S. Seidelin, D. Leibfried, J. H. Wesenberg, J. J. Bollinger, J. M. Amini, R. B. Blakestad, J. Britton, J. P. Home, W. M. Itano, J. D. Jost, E. Knill, C. Langer, R. Ozeri, N. Shiga, and D. J. Wineland, Phys. Rev. A **76**, 033411 (2007).

[12] C. Monroe, D. M. Meekhof, B. E. King, S. R. Jefferts, W. M. Itano, D. J. Wineland, and P. Gould, Phys. Rev. Lett. **75**, 4011 (1995).

[13] K. Toyoda, T. Watanabe, T. Kimura, S. Nomura, S. Haze, and S. Urabe, Phys. Rev. A **83**, 022315 (2011).

[14] D. F. V. James, Appl. Phys. B **66**, 181 (1998).

[15] Shi-Liang Zhu, C. Monroe, and L.-M. Duan, Phys. Rev. Lett. **97**, 050505 (2006).

[16] P. A. Ivanov, S. S. Ivanov, N. V. Vitanov, A. Mering, M. Fleischhauer, and K. Singer, Phys. Rev. A **80**, 060301(R) (2009).